

Experimental demonstration of twisted light's diffraction theory based on digital spiral imaging

Wuhong Zhang (张武虹), Ziwen Wu (吴自文), Jikang Wang (王继康),
and Lixiang Chen (陈理想)*

Department of Physics, College of Physics Science and Technology, Xiamen University,
Xiamen 361005, China

*Corresponding author: chenlx@xmu.edu.cn

Received May 31, 2016; accepted September 9, 2016; posted online October 17, 2016

We present both numerical and experimental results to study the diffraction of twisted light beams based on orbital angular momentum (OAM) eigenmode decomposition, where the total initial field, including light and aperture, is represented by a two-dimensional spectrum of Laguerre–Gaussian modes. We use a phase-only spatial light modulator to display a holographic grating for both generating the twisted light and mimicking the finite aperture. We take a triangular aperture as an example to describe the diffraction behavior of a twisted light beam carrying an OAM number of $\ell = 3$ from the near-field to far-field regions, where the interesting gradual formation of triangular bright lattices are observed. An excellent agreement between the numerical simulations and experimental observations is clearly seen. It is noted that this method is particularly useful for the study of the diffraction of twisted light fields incident on any apertures of rotational symmetry.

OCIS codes: 050.1940, 050.1220, 050.4865.

doi: 10.3788/COL201614.110501.

The Hermite–Gaussians (HG) modes are well known as the nearly exact eigenmodes for stable optical resonators and the normal modes of freely propagating optical beams^[1]. It has been well established that they form a complete basis set for orthogonal polynomial expansions^[2], so an arbitrary input amplitude function can be expanded in terms of HG modes and the forward traveling waves of these modes may then be used to predict the amplitude function at any diffraction distance^[3]. Like HG modes, the Laguerre–Gaussian (LG) modes also form a complete set such that they can be used for the study of light propagation based on a similar eigenmode expansion^[4–6]. Also, as was well recognized by Allen *et al.* in 1992, the LG modes were a natural candidate to describe twisted light beams carrying an orbital angular momentum (OAM) of $\ell\hbar$ per photon associated with the helical phase structure of $\exp(i\ell\phi)$, where ℓ is the OAM quantum number (or topological charge) and ϕ is the azimuth angle^[7]. Over the last two decades, light OAM has attracted great interest owing to its more and more significant applications in micromanipulation^[8,9], imaging techniques^[10–13], optical communication^[14–16], and quantum information^[17–19]. Based on the completeness of OAM eigenmodes, another fascinating application with OAM is the technique of digital spiral imaging (DSI) developed by Torner *et al.* in 2005^[20]. In this technique, a sample in the optical path scatters the beam and alters its OAM components, thus the information of the object can be extracted by analyzing the corresponding spiral spectrum, such as its spiral bandwidth or the weights of the associated OAM eigenmodes^[21]. Based on eigenmode expansion, e.g., HG and LG modes, some basic procedures have been proposed as a mathematical tool to study the light propagation and

diffraction^[22–24], which was also applied to study the radiation focusing and steering in the free-electron laser^[25,26] and to study the fiber beam characterization^[27]. However, it is noted that there is still very little research reporting both the numerical and experimental demonstrations of this theoretical method, particularly for the case with incident twisted light beams. Such an agreement between the numerical and experimental results is therefore highly desirable to confirm the reliability and effectiveness of the eigenmode decomposition method.

In addition, the rich relationship between light OAM and the far-field diffraction phenomena of single-slit^[28–31], double-slit^[32], triangular^[33–36], and multiple point-like apertures^[37] has been exploited before. The Talbot effect has also been recently used to explore the topological charges of optical vortices in the near-field regime^[38]. Specially, in 2010, Hickmann *et al.*^[33] successfully demonstrated a very elegant way to directly reveal the magnitude and sign of the topological charge of light via observing the optical lattices diffracted by a triangular aperture. We note that only the Fraunhofer diffraction pattern in the far-field region were investigated in their case, which is actually the Fourier transform of the product of the aperture and the input field functions^[39]. Here we carefully study both numerically and experimentally, based on the method of OAM eigenmode decomposition or DSI^[5,20,24], the diffraction behavior of a twisted light beam with OAM number $\ell = 3$ from a triangular aperture both in the near-field and far-field regions. An interesting evolution of diffraction patterns from the near- to far-field region is observed, which finally form the triangular bright lattice. A good agreement between numerical simulations and experimental observations is clearly seen, and therefore confirms the

feasibility of the theoretical method. This method is particularly useful for the study of twisted light diffraction by any aperture of rotational symmetry.

Our numerical simulation is based on the method of eigenmode decomposition or the idea of DSI^[5,20,24]. As is well known, the OAM eigenstates form a complete orthogonal and infinite-dimensional basis for a full Hilbert space so that we can treat any field distribution as a vector state on the basis of OAM eigenmodes, which is called by Torner *et al.* as the DSI technique^[20]. Key to the theory is that the LG modes are both the natural choice for describing twisted light carrying OAM and the solutions of the paraxial wave equation. This indicates that the diffraction of any LG beams in free space can be described just by its mathematical expression in the cylindrical coordinates (ρ, ϕ, z) , whose normalized form can be written as^[40]

$$\text{LG}(\rho, \phi, z) = \sqrt{\frac{p!}{\pi(|\ell| + p)!}} \frac{\rho^{|\ell|} \exp(i\ell\phi)}{(w^2 + iz/k)^{|\ell|+1}} \left(\frac{w^2 - iz/k}{w^2 + iz/k}\right)^p \times \exp\left(\frac{-\rho^2}{2(w^2 + iz/k)}\right) L_p^{|\ell|}\left(\frac{\rho^2}{w^2 + z^2/k^2\omega^2}\right), \quad (1)$$

where ρ is the radial cylindrical coordinate, ϕ is the azimuthal angle, z is the propagation distance, k is the wave vector, w is the beam waist, $L_p^{|\ell|}(\cdot)$ is the generalized Laguerre polynomial, and p and ℓ are the radial and azimuthal mode indices, respectively. The incident plane $z = 0$ is also the position of the given aperture. Assuming any incident structured light field is written by $u_0(\rho, \phi, z = 0)$ and an arbitrary aperture is described by its transmission function $T(\rho, \phi)$, their product can be effectively considered as the total initial field,

$$u(\rho, \phi, z = 0) = u_0(\rho, \phi, z = 0) T(\rho, \phi). \quad (2)$$

The key step to DSI is the decomposition of the initial field of Eq. (2) into a coherent superposition of the LG modes, namely,

$$u(\rho, \phi, z = 0) = \sum_{\ell=-\infty}^{+\infty} \sum_{p=0}^{+\infty} A_{\ell,p} \text{LG}_p^{\ell}(\rho, \phi, z = 0), \quad (3)$$

where $\text{LG}_p^{\ell}(\rho, \phi, z = 0)$ is given by Eq. (1) when $z = 0$. Owing to the orthogonality of LG modes, namely, $\int_0^{2\pi} d\phi \int_0^{\infty} [\text{LG}_p^{\ell}(\rho, \phi, z = 0)]^* \text{LG}_p^{\ell}(\rho, \phi, z = 0) \rho d\rho = \delta_{\ell\ell'} \delta_{pp'}$, we can calculate the spiral spectrum of the scattered beam. Each element in the spectrum is specified by

$$A_{\ell,p} = \int_0^{2\pi} d\phi \int_0^{\infty} [\text{LG}_p^{\ell}(\rho, \phi, z = 0)]^* u(\rho, \phi, z = 0) \rho d\rho, \quad (4)$$

which denotes the overlap amplitude between the relevant individual LG mode and the initial field, or the weight of the associated LG mode. With ℓ ranging from $-\ell_0$ to ℓ_0

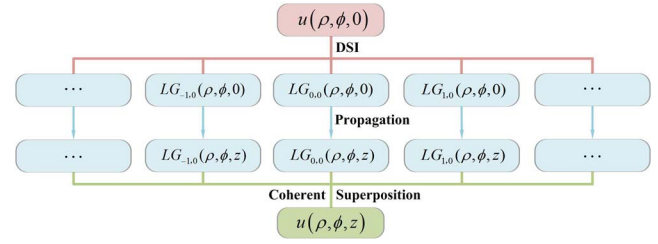


Fig. 1. Schematic of the theoretical frame based on the DSI technique (see the text for details).

and p from 0 to p_0 , $A_{\ell,p}$ is a $(2\ell_0 + 1) \times (p_0 + 1)$ complex matrix that can be equivalently represented by an intensity spectrum $|A_{\ell,p}|^2$ and a phase spectrum $\arg(A_{\ell,p})$. To calculate the diffracted field at any desired propagation distance z , we give an explanation from the physical perspective of mode decomposition, whose theoretical frame is illustrated in Fig. 1. Following the DSI technique, we can decompose the initial field in the incident plane $z = 0$, $u(\rho, \phi, 0)$, into a superposition of LG modes, as was shown by Eq. (3). According to the principle of independent propagation of light, all the LG modes contained in Eq. (3) individually propagate in free space without interplay with each other such that each mode weight indicated by Eq. (4), $A_{\ell,p}$, remains constant. Due to the superposition principle of light, the diffracted field in the desired plane z , $u(\rho, \phi, z)$, can then be treated as a consequence of a coherent superposition of all these propagating LG modes, $\text{LG}_p^{\ell}(\rho, \phi, z)$, namely,

$$u(\rho, \phi, z = 0) \rightarrow u(\rho, \phi, z) = \sum_{\ell=-\infty}^{+\infty} \sum_{p=0}^{+\infty} A_{\ell,p} \text{LG}_p^{\ell}(\rho, \phi, z), \quad (5)$$

where $A_{\ell,p}$ are given by Eq. (4). Hence, calculating the diffracted light fields at any desired plane can be simplified by changing the z coordinate from the incident plane $z = 0$ to any considered plane z for all constituent LG modes in Eq. (5). In principle, this method can be effectively applied to any incident light of arbitrary intensity/phase profile that was diffracted by any aperture of arbitrary shape, as indicated by Eqs. (2) and (3).

Our aim is to study the twisted light beam diffraction both in the near and far field based on this theory. To verify the feasibility, we consider the diffraction of twisted light beams by a triangular aperture of threefold rotational symmetry, as in the work by Hickmann *et al.*^[33]. We choose an equilateral triangular aperture, shown in Fig. 2(a), and use LabVIEW to program the superposition grating shown in Fig. 2(c). Unlike the work by Hickmann *et al.*, only studying the Fraunhofer diffraction in the far-field region, here we begin with the study in the near-field region and then change the distance z gradually to the far-field region. Compared with the Fourier method that only applies to Fraunhofer diffraction, our

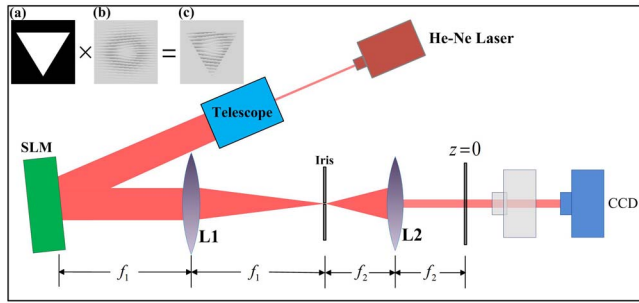


Fig. 2. Experimental setup for studying the diffraction of a twisted beam from a triangular aperture. Inset (a) is the triangular aperture, (b) is the holographic grating to produce the LG_3^0 mode, and (c) is the hologram displayed on the SLM.

demonstration shows the effectiveness of this OAM eigenmode decomposition method.

Our experimental setup is shown schematically in Fig. 2. The vertically polarized Gaussian beam derived from a 633 nm He-Ne laser is collimated by a telescope, and then is expanded and incident on the computer-controllable spatial light modulator (SLM, Hamamatsu, X10486-1). The SLM is used to generate the desired holographic grating, which contains the information of the incident OAM beam and the aperture we need. As can be seen in the inset of Fig. 2, the hologram displayed on the SLM is obtained by using a triangular aperture to multiply the modulated folk grating, which can be used to generate the standard LG beam. This design can easily ensure that the input LG beam and the triangular aperture completely coincide with each other. Here we use a $4f$ system composed of a pair of lenses whose focal lengths are $f_1 = 300$ mm and $f_2 = 150$ mm, respectively. The first-order diffracted light is selected by an iris positioned in the back focal plane of L1. Then the initial field at $z = 0$ can be imaged in the back focal plane of lens L2. Finally, the diffraction patterns at different propagation distances can be recorded by a color charge-coupled device (CCD) camera.

Following the schematic of the theoretical frame, we first plot in Fig. 3 the spiral spectra with an incident twisted beam of $\ell = 3$ and $p = 0$. The total initial field is determined by both the shape of the triangular aperture and the spiral phase profile of the incident twisted beam. After performing the mode decomposition based on Eqs. (3) and (4), we calculate both the intensity spectrum and phase spectrum, as shown in Figs. 3(a) and 3(b), respectively, where ℓ ranges from -6 to $+12$, and p from 0 to 10. It is worth noting that the threefold rotational symmetry of the triangular aperture has been well evidenced by the dominant LG components concentrated in $\ell = 3n + 3$ and around the lower-order p , where n is an integer. By summing p for each ℓ mode over all the indices, namely, $C_\ell = \sum_p |A_{\ell,p}|^2$, we then obtain a pure OAM spectrum of Fig. 3(c) that manifests the threefold symmetry more clearly. Based on Eq. (3), the total initial field with $z = 0$ is also recovered in Fig. 3(d) by using the spectrum shown in Figs. 3(a) and 3(b). One can see from

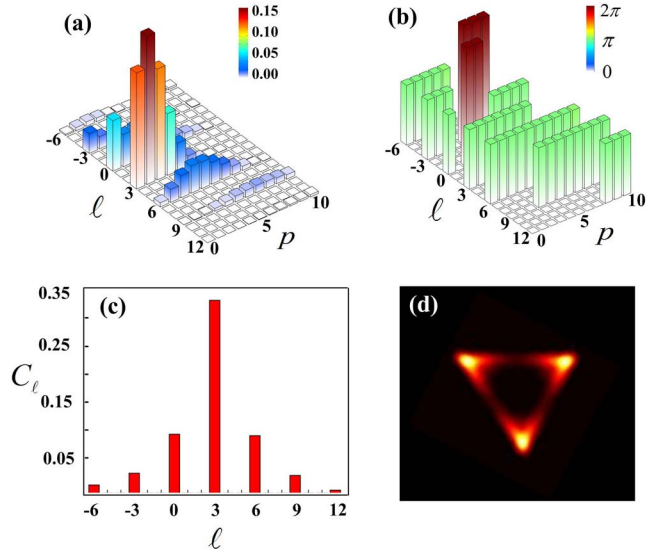


Fig. 3. Spiral spectra of the triangular aperture based on DSI. (a) Intensity spectrum $|A_{\ell,p}|^2$, (b) phase spectrum $\arg(A_{\ell,p})$ (c) ℓ spectrum $C_\ell = \sum_p |A_{\ell,p}|^2$ as a sum over all the p indices, (d) simulation results of the total initial field at the $z = 0$ plane.

Fig. 3(d) that a little aberration of the incident twisted beam is shown in the center of the triangular aperture. We attribute this issue to the use of the limited number of LG modes only with $\ell = -6$ to 12 and $p = 0$ to 10 . However, the fidelity in Fig. 3(d), defined as $F = \sum_{\ell,p} |A_{\ell,p}|^2$ can reach $F = 0.9$, implying a good similarity between the reconstructed field and the original one, which also confirms the effectiveness of the method.

Then, based on Eq. (5) with Fig. 3, we gradually increased the propagation distance from the near-incident plane, e.g., $z = 3$ cm to the far-field plane, e.g., $z = 70$ cm. We present in Fig. 4 both the simulation (top panel) and experimental results (bottom panel) of some typical diffraction patterns to illustrate the gradual birth of the triangular optical lattice. From Fig. 4, we can see that the initial three leaves of intensity maxima are gradually expanded and split into more intensity maxima. Meanwhile, after a certain propagation distance, there is a spot coming into being and growing brighter in the transverse center of the diffraction pattern. Finally, an interesting triangular bright lattice is formed with the number of

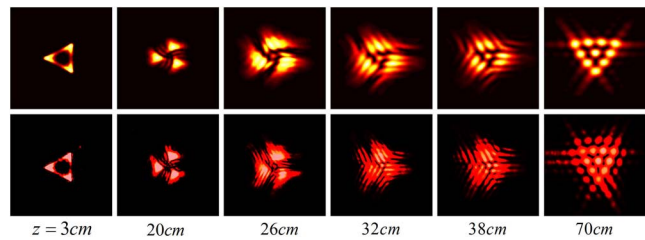


Fig. 4. Numerical (upper row) and experimental (lower row) results of diffraction of the OAM beam with $\ell = 3$, which illustrate the gradual birth of the triangular optical lattices.

its external points specified by $N = \ell + 1$, which can be used to reveal the OAM number of the incident twisted light beams^[33]. The good agreement between the experimental observations and the numerical simulations confirm that the OAM eigenmode decomposition method is a useful way to simulate the diffraction pattern of twisted light beams in a quantitative way at any propagation distance. Moreover, our study offers a more intuitive picture as to how the diffraction patterns are formed gradually from the incident plane to the desired plane. Under the condition of a known input twisted beam, the method may also be used to estimate the propagation distance and the rotational symmetry of the aperture for a given diffraction pattern, which may be very useful in OAM-based optical remote sensing.

In conclusion, we present both numerical and experimental results, as is simulated by the OAM eigenmode decomposition method or the idea of DSI, to describe the twisted light diffraction behavior both in the near-field and far-field regions. We demonstrate the gradual formation of triangular optical lattices as the light beams propagate from the incident plane to the far-field plane and also reconstruct the diffraction patterns of optical lattices in the far-field region as researchers have done before, confirming the good viability of the theoretical method. Although we only consider the cases of the incident light beams of specific OAM diffracted by a specific triangular aperture, it is noted that this method, in principle, can be applied to any incident fields of arbitrary intensity/phase profile diffracted by any apertures of arbitrary shape. In the frame of DSI, it also provides a useful understanding of light diffraction from the angle of modal decomposition, where the constituent LG modes propagate independently and contribute cooperatively to form diffraction patterns at any desired plane. This method is particularly useful to describe the twisted light diffraction with rotational symmetry.

This work was supported by the National Natural Science Foundation of China (No. 11474238), the Natural Science Foundation of Fujian Province of China for Distinguished Young Scientists (No. 2015J06002), the Fundamental Research Funds for the Central Universities at Xiamen University (Nos. 20720160040, 20720150166, and 201412G011), the Program for New Century Excellent Talents in Fujian Province University, and the program for New Century Excellent Talents in University of China (Grant No. NCET-13-0495). W. Zhang and Z. Wu contributed equally to this work.

References

1. A. E. Siegman and E. A. Sziklas, *Appl. Opt.* **13**, 2775 (1974).
2. M. Abramowitz and I. A. Stegun, *Handbook of Mathematical Functions* (Dover, 1965), Chap. 22, pp. 773.
3. H. A. Haus, *Waves and Fields in Optoelectronics* (Prentice-Hall, 1984).
4. J. Hamazaki, Y. Mineta, K. Oka, and R. Morita, *Opt. Express* **14**, 8382 (2006).
5. S. Franke-Arnold, B. Jack, J. Leach, and M. J. Padgett, *Proc. SPIE* **7227**, 72270I (2009).
6. C. Schulze, S. Ngcobo, M. Duparre, and A. Forbes, *Opt. Express* **20**, 27866 (2012).
7. L. Allen, M. W. Beijersbergen, R. J. C. Spreeuw, and J. P. Woerdman, *Phys. Rev. A* **45**, 8185 (1992).
8. D. G. A. Grier, *Nature* **424**, 810 (2003).
9. M. Padgett and L. Allen, *Phys. World* **10**, 35 (1997).
10. A. Jesacher, S. Fürhapter, S. Bernet, and M. Ritsch-Marte, *Phys. Rev. Lett.* **94**, 233902 (2005).
11. B. Jack, J. Leach, J. Romero, S. Franke-Arnold, M. Ritsch-Marte, S. M. Barnett, and M. J. Padgett, *Phys. Rev. Lett.* **103**, 083602 (2009).
12. Y. Li, H. Yang, J. Liu, L. Gong, Y. Sheng, W. Cheng, and S. Zhao, *Chin. Opt. Lett.* **11**, 021104 (2013).
13. P. Bouchal and Z. Bouchal, *Opt. Lett.* **37**, 2949 (2012).
14. Y. Zhu and F. Zhang, *Chin. Opt. Lett.* **13**, 030501 (2015).
15. J. Wang, *Photon. Res.* **4**, B14 (2016).
16. M. Zhang, P. Jia, Y. Li, T. Lei, Z. Li, and X. Yuan, *Chin. Opt. Lett.* **13**, 100502 (2015).
17. G. Molina-Terriza, J. P. Torres, and L. Torner, *Nat. Phys.* **3**, 305 (2007).
18. S. Franke-Arnold, L. Allen, and M. Padgett, *Laser Photonics Rev.* **2**, 299 (2008).
19. A. M. Yao and M. J. Padgett, *Adv. Opt. Photonics* **3**, 161 (2011).
20. L. Torner, J. P. Torres, and S. Carrasco, *Opt. Express* **13**, 873 (2005).
21. G. Molina-Terriza, L. Rebane, J. P. Torres, L. Torner, and S. Carrasco, *JEOS RP* **2**, 07014 (2007).
22. J. J. Wen and M. A. Breazeale, *J. Acoust. Soc. Am.* **83**, 1752 (1988).
23. D. Ding and X. Liu, *J. Opt. Soc. Am. A* **16**, 1286 (1999).
24. R. Ciegis, G. Silko, and A. Dementiev, *Informatika* **13**, 149 (2002).
25. C. M. Tang and P. A. Sprangle, *IEEE J. Quantum Electron.* **21**, 970 (1985).
26. P. Sprangle, A. Ting, and C. M. Tang, *Phys. Rev. A* **36**, 2773 (1987).
27. T. Kaiser, D. Flamm, S. Schürter, and M. Duparré, *Opt. Express* **17**, 9347 (2009).
28. D. P. Ghaia, P. Senthilkumaran, and R. S. Sirohi, *Opt. Laser Eng.* **47**, 123 (2009).
29. Q. S. Ferreira, A. J. Jesus-Silva, E. J. S. Fonseca, and J. M. Hickmann, *Opt. Lett.* **36**, 3106 (2011).
30. A. Y. Bekshaev, I. A. Kurka, K. A. Mohammed, and I. I. Slobodeniuk, *Ukr. J. Phys. Opt.* **16**, 17 (2015).
31. A. Y. Bekshaev, A. S. Bekshaev, and K. A. Mohammed, *Ukr. J. Phys. Opt.* **15**, 123 (2014).
32. H. I. Sztul and R. R. Alfano, *Opt. Lett.* **31**, 999 (2006).
33. J. M. Hickmann, E. J. S. Fonseca, W. C. Soares, and S. Chávez-Cerda, *Phys. Rev. Lett.* **105**, 053904 (2010).
34. A. Mourka, J. Baumgartl, C. Shanor, K. Dholakia, and E. M. Wright, *Opt. Express* **19**, 5760 (2011).
35. P. H. F. Mesquita, A. J. Jesus-Silva, E. J. S. Fonseca, and J. M. Hickmann, *Opt. Express* **19**, 20616 (2011).
36. J. G. Silva, A. J. Jesus-Silva, M. A. R. C. Alencar, J. M. Hickmann, and E. J. S. Fonseca, *Opt. Lett.* **39**, 949 (2014).
37. G. C. G. Berkhout and M. W. Beijersbergen, *Phys. Rev. Lett.* **101**, 100801 (2008).
38. P. Panthong, S. Srisuphaphon, A. Pattanapokratana, S. Chiangga, and S. Deachapunya, *J. Opt.* **18**, 035602 (2016).
39. J. W. Goodman, *Introduction to Fourier Optics*, 2nd ed. (McGraw-Hill, 1996).
40. J. Leach, M. R. Dennis, J. Courtial, and M. J. Padgett, *New J. Phys.* **7**, 55 (2005).